Performance analysis of coded OFDM on fading channels with non-ideal interleaving and channel knowledge

Magnus Sandell[†] Sarah Kate Wilson[‡] Per Ola Börjesson[†]

[†] Division of Signal Processing
Luleå University of Technology
S-971 87 Luleå
SWEDEN

[‡] School of Electrical and Computer Engineering
Purdue University
West Lafayette, IN 47907
U.S.A.

Abstract

In this paper we investigate the coded bit-error rate in an orthogonal frequency-division multiplexing (OFDM) system. The system uses a pilot-based channel estimator and the effects of non-ideal channel knowledge and non-ideal interleaving are analysed. The resulting coded bit-error rate is calculated with an analytical method proposed by Cavers and Ho. This method avoids time-consuming simulations, which is important when designing a communication system. The theoretical results are compared with simulations and a good agreement is achieved.

Contents

Chapter 1

Introduction

Orthogonal frequency-division multiplexing (OFDM) is an emerging technique for wireless communication. It is used in Europe in digital audio broadcasting (DAB) [1] and is proposed for digital video broadcasting [2]. Its resistance to multipath fading has shown it to be useful in broadcasting applications and it is currently also considered for multiuser systems [3, 4]. In those systems, a high spectral efficiency is needed to use the available bandwidth. Hence, multiamplitude modulation schemes may become necessary to use. These can be made differential [5], which, since explicit channel estimation is not necessary, simplifies the receiver. However, a penalty in the form of increased noise power is introduced, which is avoided by coherent demodulation. In that case channel estimation becomes an important part of a communication system.

Channel estimators are usually evaluated by their mean-squared error performance. However, in a communication system the average bit-error rate (BER) is a more relevant measure. The BER can be obtained by simulations but that is time consuming and offers little or no insight to the design problem of a channel estimator. Analysis tools for coded systems have existed for some time [6, 7] but these usually assume perfect channel knowledge and are not applicable in this case. In 1992, Cavers and Ho [8] derived a new method for calculating the bit-error rate of a coded system that assumes ideal interleaving but allows for non-ideal channel knowledge. In 1992 and 1996, non-ideal interleaving was analyzed in [9, 10].

The purpose of this report is to apply the general techniques mentioned above to a coded OFDM system, where we investigate the impact of channel estimation in those systems. The effects of interleaving and channel estimator complexity are analyzed and verified with simulations. This analysis will be important in the design of a channel estimator in a OFDM system since the BER curves can be obtained very quickly. Hence it is easy to vary certain parameters and almost immediately see the result without lengthy simulations.

The system model of the OFDM system we are considering is described in Section 2. The channel estimator structure and the code used are also explained there. In Section 3 the error analysis method is described for both the channel estimator and the decoder. In Section 4 the results from the analytical method are compared with simulations, and in Section 5 the results are discussed.

Chapter 2

System description

2.1 OFDM model

Figure 2.1a depicts the OFDM base-band model used in this paper. We assume that the use of a

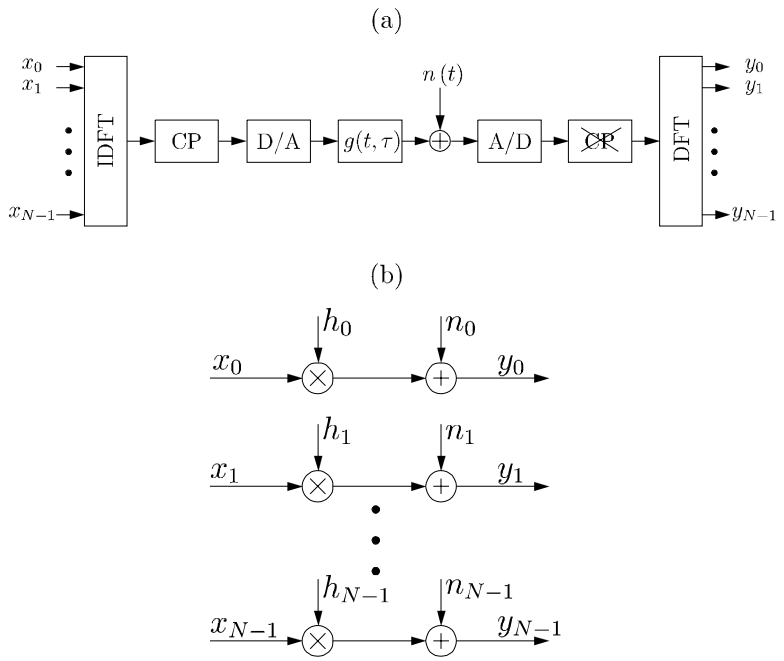

Figure 2.1: OFDM system. (a) Base-band model, (b) equivalent model.

cyclic prefix (CP) [11] both preserves the orthogonality of the tones and eliminates intersymbol interference (ISI) between consecutive OFDM symbols. Further, the channel $g(\tau; t)$ is assumed to be slowly fading, so it is considered to be constant during one OFDM symbol. The number of tones in the system is N, which makes the effective symbol length $T = NT_s$, where T_s is the sampling period of the system. The length of the cyclic prefix is $T_G = LT_s$ and the total symbol length is $T + T_G$. If the duration of the impulse response of the channel is shorter than the cyclic prefix, we can describe the system as a set of parallel Gaussian channels [12], shown in Figure 2.1b, with correlated channel attenuations h_k. The received signal on subchannel k

can thus be described as

$$y_k = h_k x_k + n_k, \tag{2.1}$$

where

$$h_k = G\left(\frac{k}{NT_s}\right),\ k = 0 \ldots N-1,$$

is the attenuation at subcarrier k and $G(\cdot)$ is the frequency response of the channel $g(t,\tau)$ during the OFDM symbol. However, it should be noted that intercarrier interference (ICI) occurs if the channel fades during an OFDM symbol [13, 14]. This ICI increases with the fading rate and for fast fading environments, this should be taken into consideration. In [14], it is shown that ICI can be modelled as Gaussian additive interference if the number of subcarriers is large. This interference is uncorrelated with the frequency response h_k. For a Rayleigh-fading channel the signal-to-interference ratio (SIR) is [14]

$$\mathrm{SIR}_{\mathrm{ICI}} = \left[1 - \frac{1}{N^2}\left(N + 2\sum_{k=1}^{N-1}(N-k)\,J_0\left(\frac{2\pi f_D k}{N}\right)\right)\right]^{-1}, \tag{2.2}$$

where f_D is the maximum Doppler frequency (relative to the intertone spacing) and $J_0(\cdot)$ is the zeroth order Bessel function of the first kind [15]. In this report the SIR is large enough to ignore intersymbol fading, see next section, and we use the simple model (2.1) without considering the ICI.

2.2 Scenario

The system we are considering is a wireless multiuser system, *e.g.* a third generation mobile telephone system. It is operating at the 2.2 GHz-band with a bandwidth of 5 MHz and 1024 subcarriers. This means that the intertone spacing is $5 \cdot 10^6/1024 = 4.88$ kHz and the symbol duration (excluding the cyclic prefix) is $1/4.88 \cdot 10^3 = 205\,\mu$s. The length of the cyclic prefix is chosen to be 50 samples, which makes the overhead equal to $50/1024 = 5$ % and the effective OFDM symbol length $205 \cdot 1.05 = 215\,\mu$s. In this report we assume perfect synchronization between transmitter and receiver. We will only deal with the downlink, where synchronization is easier, although the methods are general and are applicable to the uplink as well. The environment the system is working in is assumed to be a macrocell which can be characterized by a Rayleigh-fading channel with a Doppler frequency of 240 Hz (corresponding to 120 km/h) and a maximum time dispersion of 10 μs. Normalized to the intertone spacing and sampling interval respectively, this means $f_D = \frac{240}{5\cdot 10^6/1024} \approx 5\%$ and $\tau_{\max} = \frac{10\cdot 10^{-6}}{1/5\cdot 10^6} = 50$ samples. This Doppler rate gives us a SIR of 24 dB, see (2.2). Since we evaluate the system for SNR < 16 dB, this interference becomes negligible and we ignore the ICI caused by channel fading within an OFDM symbol.

The impulse response of the channel at time t is modelled as [16]

$$g(\tau;t) = \sum_{m=1}^{M} \alpha_m(t)\,\delta(\tau - \tau_m), \tag{2.3}$$

where the fading amplitudes $\alpha_m(t)$ are independent, complex Gaussian random variables and the delays τ_m are uniformly distributed between 0 and $\tau_{\max}$. This dispersion is shorter than

the cyclic prefix and hence ISI is avoided. The power spread profile is exponentially decaying with a root-mean-square (RMS) width of 2.2 μs = 11 samples, *i.e.*

$$E_t\left\{|g(\tau;t)|^2\right\} = \begin{cases} Ce^{-\tau/\tau_{\mathrm{rms}}} & 0 < \tau < \tau_{\max} \\ 0 & \text{otherwise} \end{cases},$$

where E_t is the expected value over t and C is a normalization constant.

2.3 Channel estimation

Pilot-symbol assisted modulation [17] has been proposed as an efficient way of combating fading. Pilot symbols, known to the receiver, are multiplexed into the transmitted symbol stream and with the aid of these, the fading channel is estimated by interpolating between the pilot symbols. For OFDM this interpolation can be done in two dimensions (time and frequency), but this usually leads to estimators with a high complexity. Therefore, separating the channel estimator into two one-dimensional estimators has been proposed [18]. First the channel attenuations on all subcarriers are estimated in only those OFDM symbols that contain pilot symbols, see Figure 2.2. Then all channel attenuations are estimated using these estimates.

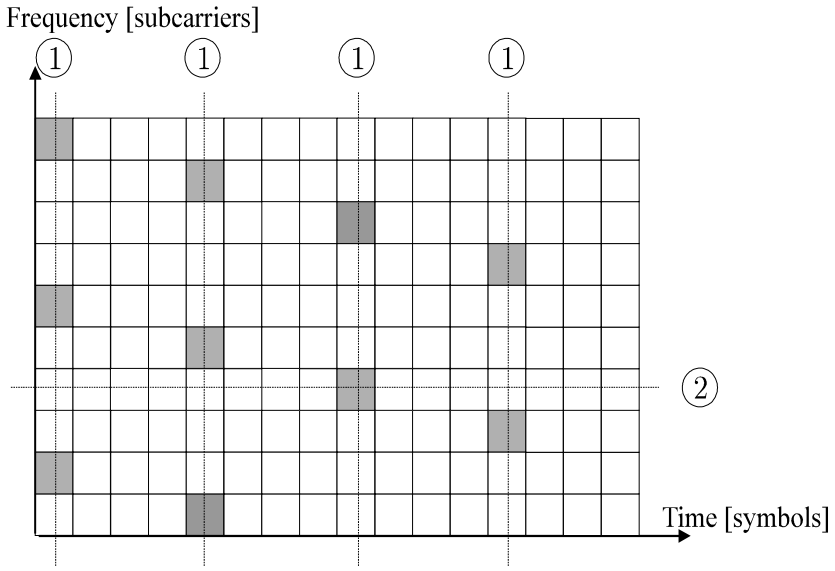

Figure 2.2: Pilot symbols, marked in gray, used for channel estimation. The channel attenuations are first estimated in the frequency direction (1) and then in the time direction (2).

The separate channel estimators can be FIR-filters [18] or low-rank estimators [19] that are designed to minimize the mean-squared error (MSE). In this report we will consider only the FIR filters. Nominal values of the channel correlation and signal-to-noise ratio (SNR) are used in order to keep the estimator fixed, which simplifies the implementation. Design for the worst case has shown to be robust and beneficial with regard to the maximum error level [17, 18, 19]. In this report we will design the estimators for a uniform power-delay profile (for $0 < \tau < \tau_{\max}$), $SNR = 30$ dB and $f_D = 5\%$. If N_f and N_t denote the number of taps in the frequency and time

filters, the average number of multiplications per attenuation is $N_f/4 + N_t$, since only every fourth OFDM symbol needs to be estimated in the frequency direction [20]. We analyze two estimators with different complexities: one with 25 taps in the frequency direction and 7 taps in the time direction and one with 5 and 2 taps, respectively. These two estimators have an average complexity of 13.25 and 3.25 multiplications per estimated attenuation, respectively.

2.4 Coding

For error protection, a convolutional code is used. To make the analysis tractable we use a rather small code with constraint length 3, which has been found to be very effective on fading channels [21]. The in-phase and quadrature signals are encoded separately with a rate 1/2 code with generator polynomials [22]:

$$\begin{aligned} g_0^{(0)}(D) &= 1 + D + D^2 \\ g_0^{(1)}(D) &= 1 + D^2. \end{aligned}$$

The encoder is depicted in Figure 2.3. The encoded outputs are modulated using 4-PAM and

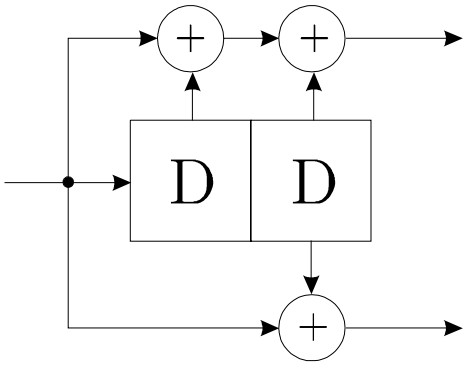

Figure 2.3: The convolutional encoder.

concatenated to a 16-QAM symbol. For a fading channel the diversity order of a code is not the free distance but the length of the shortest error event [6]. The length of an error event, L, is the number of symbols on an erroneous path that differ from the correct path. From the trellis of the code, Figure 2.4, it can be seen that the shortest error event is $L_{\min} = 3$. The receiver first equalizes the received signal y_k using the channel estimate $\widehat{h}_k$ and then separates the signal into its in-phase and quadrature parts

$$z_k = \frac{y_k}{\widehat{h}_k} = z_k^{(I)} + j z_k^{(Q)}.$$

The decoding is performed separately with the decoding metric

$$M(\widetilde{\mathbf{x}}) = \sum_k \left|\widehat{h}_k\right|^2 |\widetilde{z}_k - \widetilde{x}_k|^2, \tag{2.4}$$

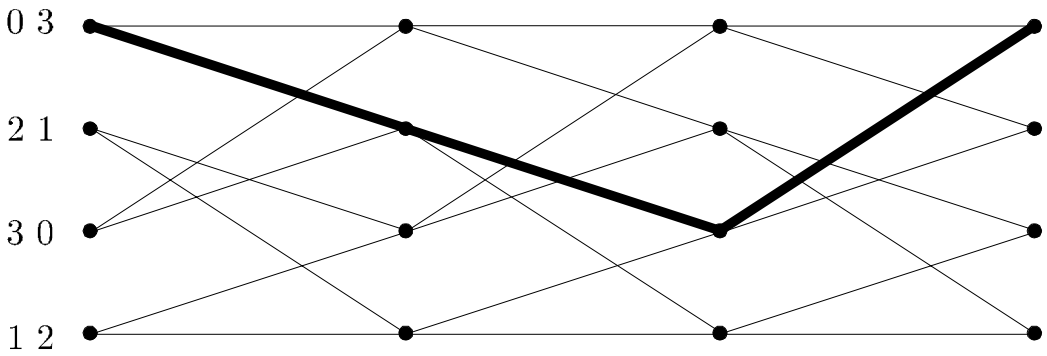

Figure 2.4: Trellis for the rate 1/2 convolutional code used. The bold path is the shortest error event.

where $\widetilde{x}_k$ is the sequence for which the metric is computed and $\widetilde{z}_k$ is either $z_k^{(I)}$ or $z_k^{(Q)}$. Using the Viterbi algorithm, the sequence $\widehat{x}_k$ which minimizes this metric is found, *i.e.*

$$\widehat{\mathbf{x}} = \arg\min_{\widetilde{\mathbf{x}}} M\left(\widetilde{\mathbf{x}}\right).$$

It should be noted that the metric in (2.4) is not the maximum-likelihood metric when multi-amplitude modulation is used [8], but we will nevertheless use it for simplicity.

In order to obtain diversity in the system from the channel code, interleaving must be used. Interleaving breaks up the channel correlation and, in the ideal case, provides the decoder with uncorrelated symbols. In this report we will use frequency interleaving on a symbol level, *i.e.* interleaving is performed after the bits have been assigned to constellation points. The symbols are block interleaved with depth D_f subcarriers across the tones. The interleaving is illustrated in Figure 2.5 with $D_f = 3$.

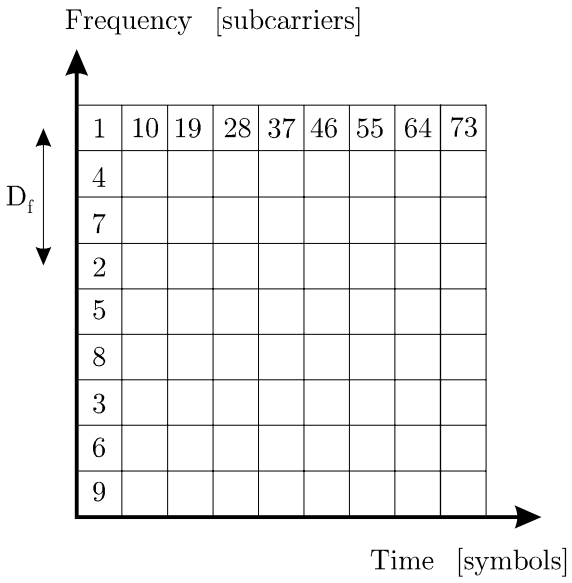

Figure 2.5: Interleaving in frequency across the tones.

In this report we assume a $M = 10$ path channel which allows the code to use its full diversity of order 3 [23]. By choosing $D_f = 128$, we have $1024/128 = 8$ symbols whose distance from each other is large enough to minimize the effects of correlation. In Figure 2.6 the frequency correlation of the channel is depicted for the scenario in this report, see Section 2.2 for parameters. Two consecutive channel symbols into the decoder have the correlation coefficient $|E\{h(m)h^*(m-128)\}|/\sigma_h^2 = 0.118$, which is small enough not to degrade the performance significantly.

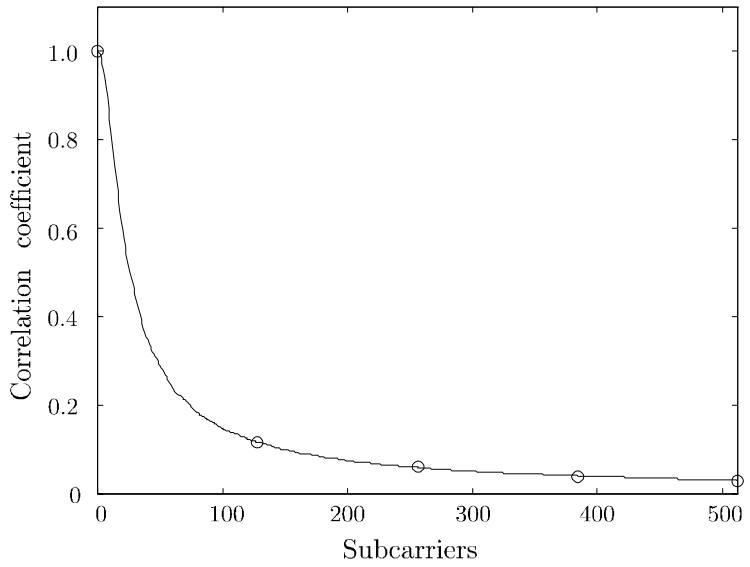

Figure 2.6: Frequency correlation for the multi-path channel. The correlations for the interleaved system ($D_f = 128$) are marked with 'o'.

Chapter 3

Performance analysis

3.1 Channel estimation

In order to evaluate a coded OFDM system, we will need four covariances from the system, see Section 3.2:

$$\begin{aligned} r_{hh}(k) &\triangleq E\left\{h(m)h^*(m-k)\right\} \\ r_{h\widehat{h}}(k) &\triangleq E\left\{h(m)\widehat{h}^*(m-k)\right\} \\ r_{\widehat{h}\widehat{h}}(k) &\triangleq E\left\{\widehat{h}(m)\widehat{h}^*(m-k)\right\} \\ r_{n\widehat{h}}(k) &\triangleq E\left\{n(m)\widehat{h}^*(m-k)\right\}. \end{aligned}$$

Notice that we assume the channel and the additive noise to be uncorrelated, $E\left\{n(m)h^*(k)\right\} = 0, \forall m, k$. How to derive explicit expressions for the above correlations is described in Appendix B.

3.2 Coding

To evaluate the probability of error for a code, one usually starts with the error event probability. An error event is defined as a path in the trellis which starts at the same node as the correct path, diverges and re-emerges some stages later with the correct path. The probability of such an error event can be upper bounded with, *e.g.,* the Chernoff bound [6, 7]. To obtain the average bit-error rate, a union bound over all error events may be applied. This enumeration of all error events can be calculated with the transfer function of the error-state diagram [6, 7] of the code. This technique, however, assumes perfect knowledge of the channel so it is not suitable for this report. We are investigating the impact of channel estimation, *i.e.*, when we do not have perfect channel knowledge. Instead, we will use the analysis introduced by Cavers and Ho [8, 21]. This technique is applicable to a more general description of the system, which includes non-ideal channel knowledge.

3.2.1 Pairwise error probability

The exact probability of an error event was found in 1992 by Cavers and Ho [8]. Assume that the decoder chooses the sequence which minimizes the metric

$$M\left(\mathbf{c}_i\right) = \sum_k \left| y_k - \widehat{h}_k c_{ik} \right|^2, \tag{3.1}$$

where $\mathbf{c}_i$ is a possible sequence of codewords and k labels the symbols *after* interleaving, *i.e.* the order in which they input to the decoder. The sequence which minimizes (3.1) can be found with the Viterbi algorithm. The probability of an error event, *i.e.* that the transmitted sequence $\mathbf{c}_i$ is decoded as $\mathbf{c}_j$ can be written as

$$\Pr\left(\mathbf{c}_i \to \mathbf{c}_j\right) = \Pr\left(M\left(\mathbf{c}_i\right) > M\left(\mathbf{c}_j\right)\right) = \Pr\left(D < 0\right), \tag{3.2}$$

where $D \triangleq M\left(\mathbf{c}_j\right) - M\left(\mathbf{c}_i\right)$ is the metric difference for the two sequences. The probability in (3.2) can be written as [21]

$$\Pr\left(D < 0\right) = -\sum \text{Residue}\left[\frac{\Phi_D(s)}{s}\right]_{\text{RHP poles}}, \tag{3.3}$$

where the sum is over the poles of $\Phi_D(s)/s$ which lies in the right halfplane of the complex plane ($\text{Re} > 0$) and $\Phi_D(s)$ is the two-sided Laplace transform of the probability distribution function of D. By rewriting D as

$$\begin{aligned} D &= M\left(\mathbf{c}_j\right) - M\left(\mathbf{c}_i\right) \\ &= \sum_k |y_k|^2 - y_k \widehat{h}_k^* c_{jk}^* - y_k^* \widehat{h}_k c_{jk} + \left|\widehat{h}_k\right|^2 |c_{jk}|^2 - \\ &\quad \sum_k |y_k|^2 - y_k \widehat{h}_k^* c_{ik}^* - y_k^* \widehat{h}_k c_{ik} + \left|\widehat{h}_k\right|^2 |c_{ik}|^2 \\ &= \sum_k y_k \widehat{h}_k^* \left(c_{ik}^* - c_{jk}^*\right) + y_k^* \widehat{h}_k \left(c_{ik} - c_{jk}\right) + \left|\widehat{h}_k\right|^2 \left(|c_{jk}|^2 - |c_{ik}|^2\right), \end{aligned} \tag{3.4}$$

we note that it is a quadratic form in the complex Gaussian variables $\left(y_k, \widehat{h}_k\right)$. Using matrix notation and denoting the length of the sequences $\mathbf{c}_i$ and $\mathbf{c}_j$ by L, (3.4) can be written as

$$D = \begin{pmatrix} y_1 \\ \vdots \\ y_L \\ \widehat{h}_1 \\ \vdots \\ \widehat{h}_L \end{pmatrix}^H \underbrace{\begin{pmatrix} 0 & \cdots & 0 & c_{i1} - c_{j1} & \cdots & 0 \\ \vdots & \ddots & \vdots & \vdots & \ddots & \vdots \\ 0 & \cdots & 0 & 0 & \cdots & c_{iL} - c_{jL} \\ c_{i1}^* - c_{j1}^* & \cdots & 0 & |c_{j1}|^2 - |c_{i1}|^2 & \cdots & 0 \\ \vdots & \ddots & \vdots & \vdots & \ddots & \vdots \\ 0 & \cdots & c_{iL}^* - c_{jL}^* & 0 & \cdots & |c_{jL}|^2 - |c_{iL}|^2 \end{pmatrix}}_{\mathbf{M}} \underbrace{\begin{pmatrix} y_1 \\ \vdots \\ y_L \\ \widehat{h}_1 \\ \vdots \\ \widehat{h}_L \end{pmatrix}}_{\mathbf{z}} = \mathbf{z}^H \mathbf{M} \mathbf{z}.$$

By using a linear transformation and an eigenvalue decomposition, see Appendix D, D can be written as [24]

$$D = \sum_{k=1}^{2L} \lambda_k |q_k|^2,$$

where q_k are independent complex Gaussian random variables, λ_k are the eigenvalues of $\mathbf{R}_{zz}\mathbf{M}$ and $\mathbf{R}_{zz} = E\left\{\mathbf{z}\mathbf{z}^H\right\}$ is the autocovariance matrix of $\mathbf{z}$. Since D is a sum of independent variables, the Laplace transform $\Phi_D(s)$ is found as [9, 25]

$$\Phi_D(s) = \prod_{k=1}^{2L} \frac{1}{1+\lambda_k s}.$$

Note that the poles of $\Phi_D(s)$ are $-1/\lambda_k$. Hence, to find the probability of a given error event in (3.3), we find the eigenvalues λ_k of the matrix $\mathbf{R}_{zz}\mathbf{M}$ and calculate the residues of $\Phi_D(s)/s$ at the poles, $-1/\lambda_k$, who lie in the right halfplane.

In the case of non-ideal interleaving, the correlation matrix $\mathbf{R}_{zz}$ is non-trivial but can be calculated as [10]

$$\mathbf{R}_{zz} = E\left\{ \begin{pmatrix} y_1 \\ \vdots \\ y_L \\ \widehat{h}_1 \\ \vdots \\ \widehat{h}_L \end{pmatrix} \begin{pmatrix} y_1 \\ \vdots \\ y_L \\ \widehat{h}_1 \\ \vdots \\ \widehat{h}_L \end{pmatrix}^H \right\} = \begin{pmatrix} E\{y_1 y_1^*\} & \cdots & E\{y_1 y_L^*\} & E\left\{y_1 \widehat{h}_1^*\right\} & \cdots & E\left\{y_1 \widehat{h}_L^*\right\} \\ \vdots & \ddots & \vdots & \vdots & \ddots & \vdots \\ E\{y_L y_1^*\} & \cdots & E\{y_L y_L^*\} & E\left\{y_L \widehat{h}_1^*\right\} & \cdots & E\left\{y_L \widehat{h}_L^*\right\} \\ E\left\{\widehat{h}_1 y_1^*\right\} & \cdots & E\left\{\widehat{h}_1 y_L^*\right\} & E\left\{\widehat{h}_1 \widehat{h}_1^*\right\} & \cdots & E\left\{\widehat{h}_1 \widehat{h}_L^*\right\} \\ \vdots & \ddots & \vdots & \vdots & \ddots & \vdots \\ E\left\{\widehat{h}_L y_1^*\right\} & \cdots & E\left\{\widehat{h}_L y_L^*\right\} & E\left\{\widehat{h}_L \widehat{h}_1^*\right\} & \cdots & E\left\{\widehat{h}_L \widehat{h}_L^*\right\} \end{pmatrix}.$$

The elements of this matrix are

$$\begin{aligned} E\{y_k y_l^*\} &= E\{(h_k x_k + n_k)(h_k x_l + n_l)^*\} = R_{hh}(k-l)x_k x_l^* + \sigma_n^2 \delta(k-l) \\ E\left\{y_k \widehat{h}_l^*\right\} &= E\left\{(h_k x_k + n_k)\widehat{h}_l^*\right\} = R_{h\widehat{h}}(k-l)x_k + R_{n\widehat{h}}(k-l) \\ E\left\{\widehat{h}_k y_l^*\right\} &= E\left\{y_l \widehat{h}_k^*\right\}^* = R_{h\widehat{h}}^*(l-k)x_l^* + R_{n\widehat{h}}^*(l-k) \\ E\left\{\widehat{h}_k \widehat{h}_l^*\right\} &= R_{\widehat{h}\widehat{h}}(k-l) \end{aligned}$$

and depend on the channel estimator used.

3.2.2 Bit-error probability

To find the average bit-error probability we can sum up all the error events (each associated with a number of information bits) to construct a union bound. This can be done with the transfer function of the code [6]. However, the error event probabilities (3.3) are not in a form suitable to use the transfer function. We will truncate the sum and only consider error events of small lengths [8]. This will not be an upper bound to the bit-error rate anymore. However, truncating the union bound can be a good approximation as argued in [8].

The average bit-error probability is approximated by

$$P_b \approx \frac{1}{n} \sum_j m_{ij} \Pr(\mathbf{c}_i \to \mathbf{c}_j),$$

where n is number of input bits per encoding interval and m_{ij} is the average number of bit-errors associated with each error event [7]. The sum is truncated to contain only error events of length $L < L_{\max}$. The maximum length $L_{\max}$ is chosen as in [21]. Define $P_b(k)$ as the estimated BER when error events of length $L \leq k$ are considered. When the increment $P_b(k+1) - P_b(k)$ is much smaller than the increments for smaller k, we choose $L_{\max} = k$. In our case we found $L_{\max} = 5$ to be a suitable choice, since considering longer error events did not change the estimated BER significantly. The error events can be enumerated using the transfer function of the error state diagram [6]. The output bits of the $(1 + D + D^2, 1 + D^2)$-code are mapped to a 4-PAM constellation. The trellis for this code along with the bit mapping for the 4-PAM constellation are shown in Figure 3.1. Note that we encode the in-phase and quadrature

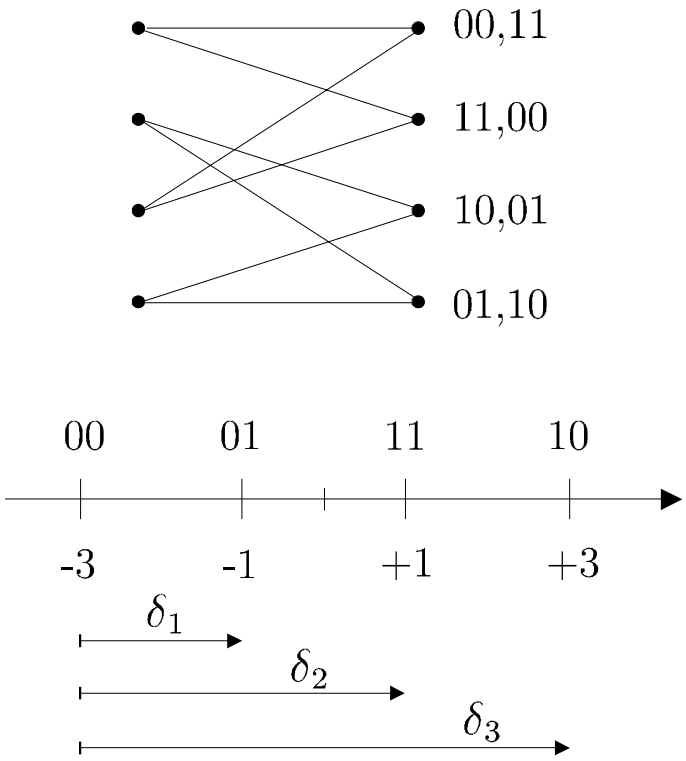

Figure 3.1: Trellis of the convolutional code and the 4PAM constellation used in the OFDM system.

dimensions separately, so for a coded 16-QAM symbol, we have two input bits and two output bits. Because we encode the in-phase and quadrature separtely, we can also analyze the two systems separately. To enumerate all error events, we use the technique described in [7, Chap. 5.3.2]. From the 4-PAM constellation, we can associate each error with a distance

$$\begin{aligned} W(00) &= 0 \\ W(01) &= \delta_1 \\ W(10) &= \frac{1}{2}(\delta_1 + \delta_3) \\ W(11) &= \delta_2. \end{aligned}$$

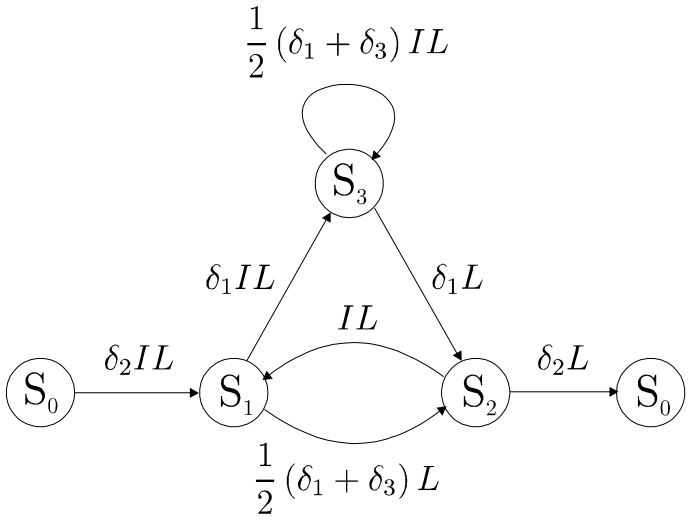

Figure 3.2: Error-state diagram for the convolutional code $(1+D+D^2, 1+D^2)$-code with 4PAM modulation.

The distance $W(10)$ may derived as follows: when the error 10 occurs, the associated distance will be δ_1 when 01 or 11 is transmitted and δ_3 when 00 or 10 is transmitted. Hence we can denote $W(10)$ by $\frac{1}{2}(\delta_1+\delta_3)$, which can be interpreted as δ_1 half of the time and δ_3 half of the time. Figure 3.2 displays the error-state diagram for this implementation of the code. Each branch in the error-state diagram is labeled by $W(\cdot)I^rL$, where $W(\cdot)$ is the Euclidean distance associated with the error, r denotes the number of information bit errors and L enumerates the branches. Using a state-space description of the error-state diagram, the error events shown in Table 3.1 can be derived (see Appendix C for the details).

Error event #	**Actual length**	**Effective length**	m_{ij}	δ_1	δ_2	δ_3
1	3	3	0.5	1	2	0
2		3	0.5	0	2	1
3	4	4	2	2	2	0
4	5	4	0.5	2	2	0
5		4	1	1	2	1
6		4	0.5	0	2	2
7		5	1.5	3	2	0
8		5	1.5	2	2	1

Table 3.1: Description of the dominating error events. The effective length is the number of symbols that differs from the transmitted codeword, m_{ij} is the average number bit errors associated with the error event, and δ_i are the Euclidean distances of the codeword symbols, see Fig. 3.1.

The effective length of a code as defined in section 3.2.2 denotes the number of channel symbols that differ in the transmitted and decoded sequence. The smallest effective length determines the diversity order of system [8]. Hence, for the code considered here we have a diversity order of 3.

Chapter 4

Simulation

4.1 Perfect channel estimation

To evalute the effect of non-ideal interleaving on our OFDM system, we apply the techniques described in section 3.2 for the case of ideal and non-ideal interleaving with perfect channel estimation. The ideal interleaving assumes that all channel attenuations are uncorrelated and the non-ideal interleaving is done as described in Section 2.4. The coding and modulation is done with the $(1 + D + D^2, 1 + D^2)$-code and 4-PAM, respectively, separately on the inphase and quadrature signals. They are then combined to form a 16-QAM symbol. In the analysis all error events of length 5 and shorter are considered. In Figure 4.1 the analytical bit-error rate curve is shown together with simulations. As can be noted from the figure, the difference between ideal and non-ideal interleaving is very small. Thus the resulting channel correlation after interleaving does not degrade the performance in any significant way.

4.2 Channel estimation

The channel estimation in these simulations is as described in Section 2.3. We first use an FIR filter to estimate the channel attenuations on all tones in a given OFDM symbol that contain pilot symbols. We then use an FIR filter in the time-domain to obtain estimates of all tones. Thus the channel estimator is a separable two-dimensional linear filter that interpolates between the initial estimates obtained at the pilot positions. The first estimator uses a 5-tap filter in the frequency direction and a 2-tap filter in the time direction, which gives an average of 3.25 multiplications per attenuation. The second estimator uses 25 and 7 taps, respectively, which results in 13.25 multiplications per attenuation. The theoretical bit-error rate for these two estimators is shown in Figure 4.2 together with the simulations. As a reference the bit-error rate with perfect channel knowledge is included.

The degradation compared to perfect channel knowledge is approximately 3 dB for the low complexity estimator and 1.3 dB for the high complexity estimator. The theoretical results show good agreement with the simulations, except for low SNR. For those low SNR values, the analytical method over-estimates the bit-error rate.

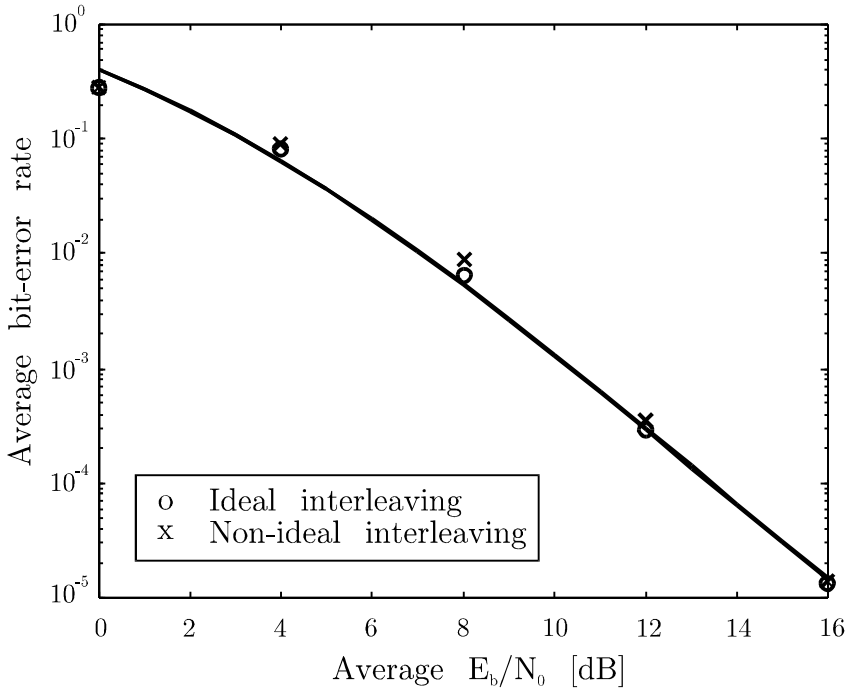

Figure 4.1: Bit-error rate with known multi-path fading channel. Simulations for ideal and non-ideal interleaving are marked with 'o' and 'x', respectively. The solid lines are the analytical results (indistinguisable for the two cases).

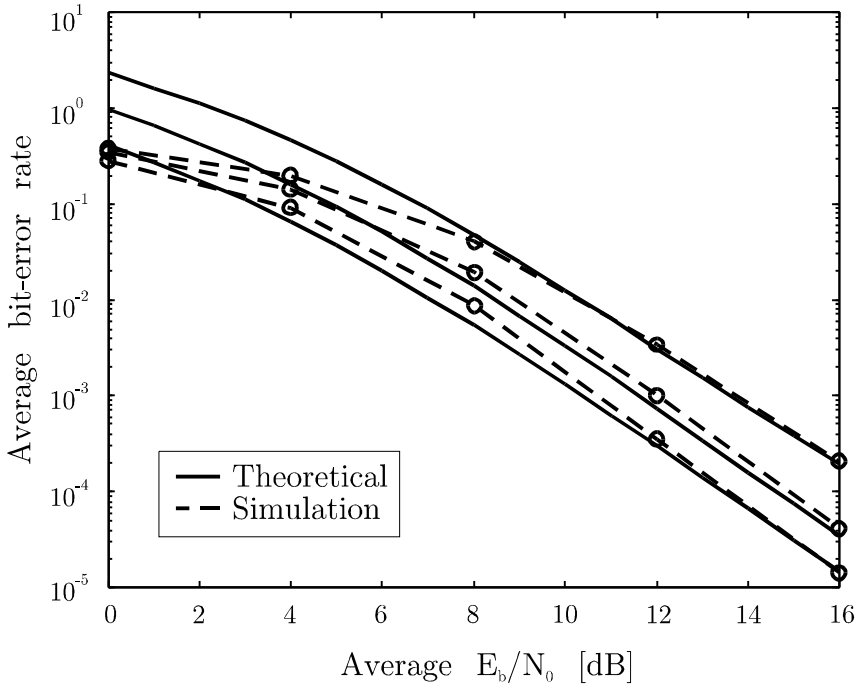

Figure 4.2: Bit-error rate for the multipath fading channel. From bottom to top: known channel, estimator A (13.25 mult./tone) and estimator B (3.25 mult./tone).

Chapter 5

Conclusions

In this report we have applied a general analysis method to a coded OFDM system. This method is most useful in the design of a system, with respect to channel estimator complexity, interleaving schemes etc., since it does not require any time-consuming simulations. Furthermore, it is general and allows the analysis to consider systems with non-ideal channel estimation and interleaving. We have investigated two versions of a channel estimator with different complexities. The lower complexity estimator is about 3 dB from the known channel, while the degradation for the higher complexity estimator is about 1.3 dB. The theoretical results agree well with simulations, except at low SNRs where it over-estimates the bit-error rate. However, for these low SNRs, the difference between the different estimators is not interesting from a design point of view as all the estimators give approximately the same bit-error rate. Thus the investigated method shows a high potential for use in the design phase of coded OFDM systems, since it is fast, simple and accurate. In this report we have only considered the effect of channel estimation, but other parameters can also be investigated, such as pilot density, choice of code, etc.

Appendix A

Channel correlation

The frequency response of the channel model in (2.3) is

$$h\left(f;t\right)=\sum_{m=1}^{M}\alpha_m\left(t\right)e^{-j2\pi f\tau_m}$$

and the frequency correlation between two attenuations spaced l subcarriers apart is

$$\begin{aligned}R_{\text{freq}}\left(l\right) &= E\left\{h\left(\frac{k}{NT_s};t\right)h^*\left(\frac{k-l}{NT_s};t\right)\right\}=E\left\{\sum_{m=1}^{M}\left|\alpha_m\left(t\right)\right|^2e^{-j2\pi l\tau_m/NT_s}\right\}\\ &= \frac{1}{LT_s}\sum_{m=1}^{M}\int_0^{LT_s}Ce^{-\tau_m/\tau_{\text{rms}}}e^{-j2\pi l\tau_m/NT_s}d\tau_m\\ &= CM\cdot\frac{1-\exp\left(-\frac{LT_s}{\tau_{\text{rms}}}-j2\pi l\frac{L}{N}\right)}{\frac{LT_s}{\tau_{\text{rms}}}+j2\pi l\frac{L}{N}},\end{aligned}$$

where the normalization coefficient C is chosen such that $R_{\text{freq}}\left(0\right)=1$. The channel estimator is designed for a uniform power delay profile, which can be obtained when $\tau_{\text{rms}}\to\infty$,

$$R_{\text{freq,uniform}}\left(l\right)=\frac{CM}{j2\pi l\frac{L}{N}}\left(1-\exp\left(-j2\pi l\frac{L}{N}\right)\right).$$

The time variation of the channel follows Jakes' model [15], whose time correlation is $R\left(t\right)=J_0\left(2\pi F_Dt\right)$, where $J_0\left(\cdot\right)$ is the zeroth order Bessel function of the first kind and F_D is the maximum Doppler frequency. Thus the correlation between two attenuations with a distance of m OFDM symbols is

$$R_{\text{time}}\left(m\right)=J_0\left(2\pi F_Dm\left(N+L\right)T_s\right)=J_0\left(2\pi f_Dm\left(1+\frac{L}{N}\right)\right),$$

where f_D is the relative (to the intertone spacing) maximum Doppler frequency.

Appendix B

Channel estimator

The channel estimator used here is a separable Wiener filter [18]. Consider first the channel estimation in the frequency direction. In those OFDM symbols where there are pilots, these estimates are

$$\widetilde{h}^{(i)}(k,l) = \sum_m \alpha_m^{(i)} \widehat{h}_{\mathrm{ls}}(k - mN_f - i, l), \; i = 0, \ldots, N_f - 1,$$

where (k,l) denotes subcarrier k at symbol l, superscript (i) indicates that the estimated attenuation lies i subcarriers from a pilot and N_f is the distance between pilot symbols. Note that pilots are placed at $i = 0$ and that we need N_f different estimators $\alpha_m^{(i)}$ since the estimated attenuations are placed differently relative to the pilots. These preliminary estimates are then used for the estimation in the time direction:

$$\begin{aligned} \widehat{h}_{k,l}^{(i,j)} &= \sum_n \beta_n^{(j)} \widetilde{h}^{(i)}(k, l - nN_t - j), \; j = 0, \ldots, N_t - 1 \\ &= \sum_{m,n} \alpha_m^{(i)} \beta_n^{(j)} \widehat{h}_{\mathrm{ls}}(k - mN_f - i, l - nN_t - j). \end{aligned}$$

Here the superscript (j) denotes the distance between the estimated attenuation and an OFDM symbol with pilots. By placing all the used pilots in a vector $\mathbf{p}$, the estimator may be expressed as

$$\widehat{h}_{k,l}^{(i,j)} = \mathbf{g}_{i,j}^T \mathbf{p}_{k-i,l-j},$$

where

$$\mathbf{g}_{i,j} = \begin{pmatrix} \alpha_{m_{\min}}^{(i)} \beta_{n_{\min}}^{(j)} \\ \vdots \\ \alpha_{m_{\max}}^{(i)} \beta_{n_{\min}}^{(j)} \\ \alpha_{m_{\min+1}}^{(i)} \beta_{n_{\min}}^{(j)} \\ \vdots \\ \alpha_{m_{\max}}^{(i)} \beta_{n_{\max}}^{(j)} \end{pmatrix}, \; \mathbf{p}_{k,l} = \begin{pmatrix} \widehat{h}_{\mathrm{ls}}(k - m_{\min}N_f, l - n_{\min}N_t) \\ \vdots \\ \widehat{h}_{\mathrm{ls}}(k - m_{\max}N_f, l - n_{\min}N_t) \\ \widehat{h}_{\mathrm{ls}}(k - m_{\min}N_f, l - n_{\min+1}N_t) \\ \vdots \\ \widehat{h}_{\mathrm{ls}}(k - m_{\max}N_f, l - n_{\max}N_t) \end{pmatrix}.$$

From this description it is straightforward to obtain the correlations needed for the analysis. Due to the periodic pattern of the pilots there will be $N_f N_t$ different estimators, all with different performance. Hence we average over all estimated attenuation to get a scalar parameter.

For instance, the cross-correlation between the channel and the channel estimate is set to be

$$R_{h\widehat{h}}\left(k,l;k',l'\right)=\frac{1}{N_f N_t}\sum_{i,j}E\left\{h_{k,l}\widehat{h}^{(i,j)}_{k',l'}\right\}.$$

This can be justified in that there is only a small variation among the estimated attenuations and they have all approximately the same properties. Note that the correlations should be calculated *after* de-interleaving and that the indices of the variables should be adjusted accordingly.

Appendix C

Error event enumeration

The error-state diagram for the $(1 + D + D^2, 1 + D^2)$-code with 4-PAM modulation considered in this report is depicted in Figure 3.2. To calculate the transfer function of the error-state diagram we use a state-space description [6]:

$$\begin{pmatrix} \xi_1 \\ \xi_2 \\ \xi_3 \end{pmatrix} = \underbrace{\begin{pmatrix} 0 & IL & 0 \\ \frac{1}{2}(\delta_1 + \delta_3) L & 0 & \delta_1 L \\ \delta_1 IL & 0 & \frac{1}{2}(\delta_1 + \delta_3) L \end{pmatrix}}_{\mathbf{A}} \begin{pmatrix} \xi_1 \\ \xi_2 \\ \xi_3 \end{pmatrix} + \underbrace{\begin{pmatrix} \delta_2 IL \\ 0 \\ 0 \end{pmatrix}}_{\mathbf{B}} \xi_{\text{in}}$$

$$\xi_{\text{out}} = \underbrace{\begin{pmatrix} 0 & \delta_2 L & 0 \end{pmatrix}}_{\mathbf{C}} \begin{pmatrix} \xi_1 \\ \xi_2 \\ \xi_3 \end{pmatrix}$$

The transfer function is

$$\frac{\xi_{\text{out}}}{\xi_{\text{in}}} = \mathbf{C}\left(\mathbf{I} - \mathbf{A}\right)^{-1}\mathbf{B}$$

By noting that $(\mathbf{I} - \mathbf{A})^{-1} = \sum_{k=0}^{\infty} \mathbf{A}^k$, and that all matrices contain the scalar L, the transfer function can be written as

$$\frac{\xi_{\text{out}}}{\xi_{\text{in}}} = \sum_{k=0}^{\infty} \widetilde{\mathbf{C}}\widetilde{\mathbf{A}}^k\widetilde{\mathbf{B}}L^{k+2}$$

where $\mathbf{A} = L\widetilde{\mathbf{A}}$, $\mathbf{B} = L\widetilde{\mathbf{B}}$ and $\mathbf{C} = L\widetilde{\mathbf{C}}$. Hence, $\xi_{\text{out}}/\xi_{\text{in}}$ is a polynomial in L and all error events of length $k+2$ can be found as $\widetilde{\mathbf{C}}\widetilde{\mathbf{A}}^k\widetilde{\mathbf{B}}$. This can now be used to find all dominant error events.

Appendix D

Laplace transform $\Phi_D(s)$

This derivation of the Laplace transform of the quadratic form D follows Turin [25] and Mazo and Salz [24]. The quadratic form

$$D = \mathbf{z}^H \mathbf{M} \mathbf{z}$$

is easier to work with if we make the elements in $\mathbf{z}$ uncorrelated, *i.e.*, $\mathbf{p} = \mathbf{R}_{zz}^{-1/2}\mathbf{z}$. Now we have $E\left\{\mathbf{p}\mathbf{p}^H\right\} = E\left\{\mathbf{R}_{zz}^{-1/2}\mathbf{z}\mathbf{z}^H\mathbf{R}_{zz}^{-1/2}\right\} = \mathbf{I}$ which is the identity matrix. Note that $\mathbf{R}_{zz}$ is Hermitian, *i.e.*, $\mathbf{R}_{zz} = \mathbf{R}_{zz}^H$. From the new quadratic form

$$D = \mathbf{p}^H \mathbf{R}_{zz}^{1/2} \mathbf{M} \mathbf{R}_{zz}^{1/2} \mathbf{p}$$

we do an eigenvalue decomposition

$$\mathbf{R}_{zz}^{1/2} \mathbf{M} \mathbf{R}_{zz}^{1/2} = \mathbf{U} \mathbf{\Lambda} \mathbf{U}^H,$$

where $\mathbf{U}$ contains the eigenvectors and $\mathbf{\Lambda} = \text{diag}\left(\begin{array}{ccc} \lambda_1 & \cdots & \lambda_{2L} \end{array}\right)$ is a diagonal matrix with the eigenvalues. The quadratic form is now

$$D = \mathbf{p}^H \mathbf{U} \mathbf{\Lambda} \mathbf{U}^H \mathbf{p} = \mathbf{q}^H \mathbf{\Lambda} \mathbf{q} = \sum_{k=1}^{2L} \lambda_k \left|q_k\right|^2,$$

where $\mathbf{q} = \mathbf{U}^H \mathbf{p}$ contains uncorrelated elements since $\mathbf{U}$ is an unitary matrix [26]. Thus q_k are independent complex Gaussian variables with unit variance. Since the real and imaginary part of q_k are independent, $\lambda_k \left|q_k\right|^2$ is χ^2 (2)-distributed with corresponding Laplace transform $\left(1 + \lambda_k s\right)^{-1}$ [27]. The Laplace transform of a sum of independent variables is the product of their individual transforms [27] and hence,

$$\Phi_D(s) = \prod_{k=1}^{2L} \frac{1}{1 + \lambda_k s}.$$

Note that the eigenvalues λ_k of $\mathbf{R}_{zz}^{1/2} \mathbf{M} \mathbf{R}_{zz}^{1/2}$ are the eigenvalues of $\mathbf{R}_{zz}\mathbf{M}$:

$$\begin{aligned} \det\left(\mathbf{R}_{zz}^{1/2} \mathbf{M} \mathbf{R}_{zz}^{1/2} - \lambda \mathbf{I}\right) &= \det\left(\mathbf{R}_{zz}^{-1/2}\left(\mathbf{R}_{zz}\mathbf{M} - \lambda \mathbf{I}\right)\mathbf{R}_{zz}^{1/2}\right) = \\ \det\left(\mathbf{R}_{zz}^{-1/2}\right) \det\left(\mathbf{R}_{zz}\mathbf{M} - \lambda \mathbf{I}\right) \det\left(\mathbf{R}_{zz}^{1/2}\right) &= \det\left(\mathbf{R}_{zz}\mathbf{M} - \lambda \mathbf{I}\right). \end{aligned}$$

Bibliography

[1] Radio broadcasting systems; Digital Audio Broadcasting (DAB) to mobile, portable and fixed receivers. ETS 300 401, ETSI – European Telecommunications Standards Institute, Valbonne, France, February 1995.

[2] Digital broadcasting systems for television, sound and data services. European Telecommunications Standard, prETS 300 744 (Draft, version 0.0.3), April 1996.

[3] C. Reiners and H. Rohling. Multicarrier transmission technique in cellular mobile communication systems. In *Proc. IEEE Vehic. Technol. Conf.*, pages 1645–1649, Stockholm, Sweden, June 1994.

[4] H. Rohling and R. Grünheid. Multicarrier transmission technique in mobile communication systems. In *Proc. RACE Mobile Commun. Summit*, pages 270–276, Cascais, November 1995.

[5] Volker Engels and Hermann Rohling. Multilevel differential modulation techniques (64-DAPSK) for multicarrier transmission systems. *Eur. Trans. Telecommun. Rel. Technol.*, 6(6):633–640, November 1995.

[6] Ezio Biglieri, Dariush Divsalar, Peter J. McLane, and Marvin K. Simon. *Introduction to trellis-coded modulation with applications*. Macmillan, New York, 1991.

[7] S. Hamidreza Jamali and Tho Le-Ngoc. *Coded-modulation techniques for fading channels*. Kluwer Academic Publishers, 1994.

[8] James Cavers and Paul Ho. Analysis of the error performance of trellis-coded modulation in Rayleigh-fading channels. *IEEE Trans. Commun.*, 40(1):74–83, January 1992.

[9] Paul Ho and Dominic Fung. Error performance of interleaved trellis-coded PSK modulations in correlated Rayleigh-fading channels. *IEEE Trans. Commun.*, 40(12):1800–1809, December 1992.

[10] Robert van Nobelen and Desmond P. Taylor. Analysis of the pairwise error probability of noninterleaved codes on the Rayleigh-fading channel. *IEEE Trans. Commun.*, 44(4):456–463, April 1996.

[11] A. Peled and A. Ruiz. Frequency domain data transmission using reduced computational complexity algorithms. In *Proc. IEEE Int. Conf. Acoust., Speech, Signal Processing*, pages 964–967, Denver, CO, 1980.

[12] John A. C. Bingham. Multicarrier modulation for data transmission: An idea whose time has come. *IEEE Commun. Mag.*, 28(5):5–14, May 1990.

[13] A. Müller. OFDM transmission over time-variant channels. In *Proc. Int. Broadc. Conv.*, number 397, pages 533–538, Amsterdam, Netherlands, September 1994.

[14] Mark Russell and Gordon Stüber. Interchannel interference analysis of OFDM in a mobile environment. In *Proc. IEEE Vehic. Technol. Conf.*, volume 2, pages 820–824, Chicago, IL, July 1995.

[15] William C. Jakes. *Microwave mobile communications*. Classic Reissue. IEEE Press, Piscataway, New Jersey, 1974.

[16] J.G. Proakis. *Digital communications*. Prentice-Hall, 3rd edition, 1995.

[17] James K. Cavers. An analysis of pilot-symbol assisted modulation for Rayleigh-fading channels. *IEEE Trans. Vehic. Technol.*, 40(4):686–693, November 1991.

[18] Peter Höher. TCM on frequency-selective land-mobile fading channels. In *Proc. Tirrenia Int. Workshop Digital Commun.*, Tirrenia, Italy, September 1991.

[19] Ove Edfors, Magnus Sandell, Jan-Jaap van de Beek, Sarah Kate Wilson, and Per Ola Börjesson. OFDM channel estimation by singular value decomposition. Research Report TULEA 1996:18, Div. of Signal Processing, Luleå University of Technology, September 1996.

[20] Magnus Sandell and Ove Edfors. A comparative study of pilot-based channel estimators for wireless OFDM. Research Report TULEA 1996:19, Div. of Signal Processing, Luleå University of Technology, September 1996.

[21] Paul Ho, James Cavers, and Jean Varaldi. The effects of constellation density on trellis-coded modulation in fading channels. *IEEE Trans. Vehic. Technol.*, 42(3):318–325, August 1993.

[22] Stephen G. Wilson. *Digital modulation and coding*. Prentice-Hall, New Jersey, USA, 1996.

[23] Sarah Kate Wilson. *Digital audio broadcasting in a fading and dispersive channel*. PhD thesis, Stanford University, CA, August 1994.

[24] J. Mazo and J. Salz. Probability of error for quadratic detectors. *Bell System Tech. J.*, 44(9):2165–2185, November 1965.

[25] George L. Turin. The characteristic function of Hermitian quadratic forms in complex normal variables. *Biometrika*, 47:199–201, 1960.

[26] Gilbert Strang. *Linear Algebra and Its Applications*. Academic Press, 2nd edition, 1980.

[27] G.R. Grimmett and D.R. Stirzaker. *Probability and random processes*. Oxford University Press, Oxford, England, 2nd edition, 1992.